專　論

飽和破碎層中現地延散係數之現場測定

In-Situ Determination of Field-Scale Dispersion Coefficients in Saturated Fractured Formations

國立臺灣大學農業工程學系客座教授
衞　紹　騏
Shao-Chih Way

美國 In-Situ Inc. 董事長
馬基卡斯特
Chester R. McKee

摘　　要

研究地下水污染的傳動問題中，延散係數爲一重要之水力參數，通常在實驗室所量測試體之延散係數遠較現地所量測之延散係數爲小。

本文目的在闡明使用 de Josselin de Jong 之理論及現地追蹤實驗方法來決定飽和破碎層中之現地延散係數，此方法需在地層上游建立一注入井，並在下游至少設置一觀測井。在觀測井量測注入井注入之追蹤劑的濃度變化，可以繪成一時間—濃度之特性曲線，藉由該特性曲線以求得現地之延散係數，本方法之特點爲：

(1)本追蹤試驗使用地下水之天然水力梯度，在試驗中不回注或抽取，以免造成人工水力梯度。

(2)本方法不僅可測定縱向延散係數，亦可測定橫向延散係數，及兩者間之方向性關係。

本方法成功的應用在美國華盛頓林肯郡之現地追蹤實驗之井羣中。

ABSTRACT

One of the most important hydraulic parameters in dealing with the transport of contaminants in groundwater is dispersivity. The laboratory-measured dispersivity on a core is usually orders of magnitude smaller than the field-scale dispersivity.

This paper presents a field tracer test method, using the theory of de Josselin de Jong, to determine field-scale dispersion coefficients in saturated fractured formations. The method requires one upstream injection well and at least one downstream observation well. The characteristics of the time-concentration curve observed in the observation well, as the result of a tracer released in the injection well, are used to analyze for dispersion coefficients. The important aspects of this method are (1) the tracer test is performed in a natural groundwater system, with no induced injection or pumping during the test; (2) the method will provide information not only on longitudinal dispersion coefficient, but also on transverse dispersion coefficient, and the directions of each. The method was successfully applied in a tracer test performed on a research wellfield near Creston in Lincoln County, Washington, U.S.A.

INTRODUCTION

Dispersion exhibits unique behavior in fractured rock units. Fracture characteristics govern dispersion and the direction of plume movement. Contrary to conventional assumptions about dispersion, the movement of the plume in fractured rock does not necessarily follow the direction of hydraulic gradient; and the direction of longitudinal dispersion may deviate from the direction of plume movement.

Dispersion in fractured formations is also a scale-dependent parameter. The basic reason for scale dependence is that a fractured medium generally exhibits small fractures (on a scale of centimeters), separated by major fractures with spacing on the order of meters or tens of meters, and finally by faults with intervals in the range of hundreds of meters and even kilometers. As a result, dispersion would initially begin with solute spreading into small-scale fractures. Progressing downstream, it would successively migrate into ever larger fractures. Since dispersivity is proportional to the fracture intersection length, the dispersivity would therefore progressively increase as spreading continues and then attain a constant value consistent with the intersection frequency of the main flow channels in the aquifer.

Three approaches are generally employed in studying dispersion. The first is that of Bear and Bachmat,[1] who statistically averaged over the medium's conductance and tortuosity to arrive at a fourth-rank tensor, which when multiplied with a second-rank tensor product of average velocities results in a second-rank dispersivity tensor.

The second approach uses statistical descriptions of the medium's hydraulic conductivity to derive expressions for the dispersion coefficient. These are exemplified by Gelhar, Gutjahr, and Naff;[2] Gelhar and Axness;[3] and Winter, Neuman, and Newman.[4] Neuman, Winter, and Newman[5] later presented a three-dimensional theory to describe field-scale Fickian dispersion in anisotropic porous media.

The third approach uses measurement of joint and fracture sets to construct a network of fractures or can include a probability distribution. Together with the conductivity tensor and the vector hydraulic gradient, dispersion coefficients may be calculated exactly. This method is found in the publications of de Josselin de Jong,[6,7,8] de Josselin de Jong and Way,[9] and Way and McKee.[10] This method is realistic for fractured systems in that a tracer particle travels a discrete length, which may be variable, before branching to another flow path.

A field tracer test procedure using de Josselin de Jong's theory[8] is proposed to determine field-scale dispersion coefficients in saturated fractured formations. The proposed method offers the following advantages over other methods:

1. The tracer test is conducted in an undisturbed natural groundwater system. Only one slug of tracer is released from the upstream injection well and travels with the natural groundwater flow. There is no induced pumping or injection. Reliable field-scale dispersion effects can be examined.
2. Only one upstream injection well is required, and, with sufficient knowledge of groundwater flow, only one downstream observation well.
3. With the availability of downhole specific-conductivity probes and automatic data loggers, performance of long-term (several months) passive tracer tests becomes economically feasible.
4. This method is applicable in anisotropic media, especially in fractured formations, where the direction of longitudinal dispersion is usually not parallel to the direction of groundwater flow.
5. The method provides information not only on longitudinal dispersion, but also on transverse dispersion and the respective directions of each.

The application of the proposed method was demonstrated successfully in a tracer test performed on a research wellfield near Creston, Washington.

THEORY

In saturated fractured formations, the concentration distribution C(X, Y, Z, T) due to the injection of a total amount of tracer mass M, at a point X=0, Y=0, Z=0, and time, T, in an

anisotropic porous medium is (de Josselin de Jong,[8] eq. 12.2):

$$C(X,Y,Z,T) = \frac{M}{\eta}\sqrt{\frac{||B||\langle t\rangle^3}{(2\pi T)^3}}\exp\left\{-\frac{1}{2}B_{kl}\frac{\langle t\rangle}{T}\left[X_k - \frac{\langle x_k\rangle}{\langle t\rangle}T\right]*\left[X_l - \frac{\langle x_l\rangle}{\langle t\rangle}T\right]\right\}, \quad (1)$$

where

C =concentration of injected tracer [ML^{-3}]

X,Y,Z =rectangular coordinates [L]

M =mass of injected tracer [M]

η =effective porosity

T =time [T]

$\langle x\rangle$ =average of x [L]

$\langle t\rangle$ =average of t [T]

B_{kl} =is related to dispersion-coefficient tensor D_{ik} by Eq. 2, and

$||B||$ =is the determinant of tensor B_{kl} [L^{-2}].

$$D_{ik}\,B_{kl}\langle t\rangle = \frac{1}{2}\delta_{il}, \quad (2)$$

where subscripts i,k,l represent a set of coordinate systems. δ_{il} is Kroneker delta, where

$\delta_{il} = 1$ for $i = 1$,

$\delta_{il} = 0$ for $i \neq 1$.

The probability distribution is related to the tracer concentration by:

$$P(X,Y,Z,T) = C(X,Y,Z,T)\,\eta/M. \quad (3)$$

Eq. 1 therefore becomes

$$P(X,Y,Z,T) = \sqrt{\frac{||B||\langle t\rangle^3}{(2\pi T)^3}}\exp\left\{-\frac{1}{2}B_{kl}\frac{\langle t\rangle}{T}\left[X_k - \frac{\langle x_k\rangle}{\langle t\rangle}T\right]*\left[X_l - \frac{\langle x_l\rangle}{\langle t\rangle}T\right]\right\}. \quad (4)$$

In the two-dimensional case, Eq. 4 can be simplified to three independent equations (Eqs. 5, 6, and 7) by assuming that the tracer concentration expressed in Eq. 4 is a Gaussian approximation with respect to time (see Appendix for detailed derivations).

$$\frac{T^A}{2(\sigma^A)^2} = \frac{1}{4||D||}\left[D_{xx}\langle v_y\rangle^2 - 2D_{xy}\langle v_x\rangle\langle v_y\rangle + D_{yy}\langle v_x\rangle^2\right] \quad (5)$$

$$\frac{(T^A)^3}{2(\sigma^A)^2} = \frac{1}{4||D||}\left[D_{xx}(Y^A)^2 - 2D_{xy}X^AY^A + D_{yy}(X^A)^2\right] \quad (6)$$

$$C^A_{peak}(2\pi T^A)\exp\left\{\left[\frac{T^A}{\sigma^A}\right]^2\right\} = \frac{M}{\eta}\left(4||D||\right)^{-1/2} * \exp\left\{\frac{\left[D_{xx}\langle v_y\rangle Y^A - D_{xy}\left[\langle v_y\rangle X^A + \langle v_x\rangle Y^A\right] + D_{yy}\langle v_x\rangle X^A\right]}{2||D||}\right\}, \quad (7)$$

where

T^A=elapsed time for the peak tracer concentration to reach downstream observation well A (Fig. 1),

σ^A=time increment of concentration standard deviation observed at downstream observation well A (Fig. 1),

C^A_{peak}=peak tracer concentration observed at downstream observation well A (Fig. 1),

D_{xx}, D_{xy}, D_{yy}=components of dispersion coefficient,

$||D||$=determinant of dispersion coefficient,

$\langle V_x\rangle\langle V_y\rangle$ =x and y components of groundwater velocity,

X^A, Y^A=x and y coordinates of downstream observation well A.

Whether the shape of the concentration profile satisfies a Gaussian approximation has been a point of discussion by several authors.[5,11,12,13] Eqs. A 14 and A. 15 in the Appendix suggest that Gaussian approximation improves with time. Sudicky et al.[14] provide an excellent example showing that concentration profiles of dispersion plumes approached a Gaussian distribution with time in a real field study.

Eqs. 5, 6, and 7 provide the theoretical basis for determination of field-scale dispersion coefficients in saturated fractured formations.

PROCEDURE

1. Drill at least two wells to the formation of interest. Use the upstream well as an injection well and the downstream well as an observation well. (At least three wells are needed to obtain hydraulic gradient.)
2. Inject a slug of non-absorbing tracer of mass M into the injection well.
3. Record time-concentration profile data collected at Well A (X^A, Y^A) (Fig. 1). The time-concentration curve will have the characteristics of C^A_{peak}, T^A, and σ^A, as indicated in Fig. 1.
4. Use Darcy's Law to calculate $\langle V_x \rangle$, $\langle V_y \rangle$, and η.
5. Assume a value for $||D||$, where

$$||D|| = D_{xx}D_{yy} - D_{xy}^2. \quad (8)$$

Calculate

$$E1 = \frac{2T^A}{[\sigma^A]^2}||D|| \quad (9)$$

$$E2 = \frac{2[T^A]^3}{[\sigma^A]^2}\cdot||D|| \quad (10)$$

$$E3 = 2||D|| \ln\left\{\left[4||D||\right]^{1/2} * C^A_{peak}\left[2\pi T^A\right]\frac{\eta}{M}\exp\left[\left|\frac{T^A}{\sigma^A}\right|^2\right]\right\} \quad (11)$$

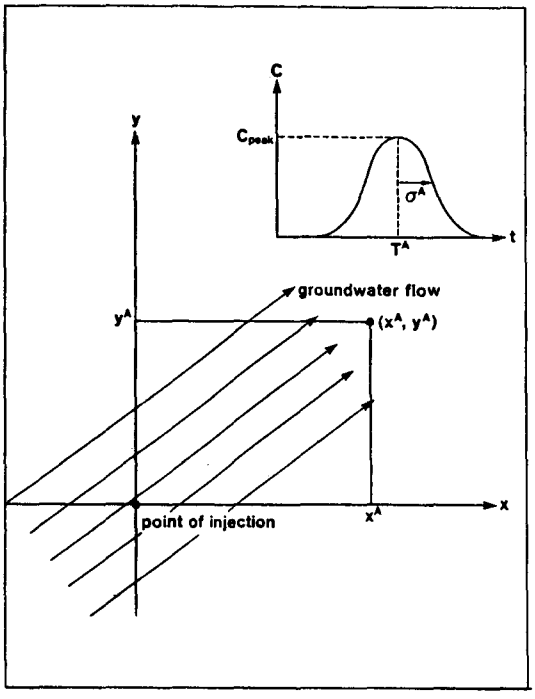

Fig. 1. Concentration plume at $X=X^A$ and $Y=Y^A$

6. Solve for D_{xx}, D_{xy}, and D_{yy}, as follows:

$$D_{xx}\langle V_y\rangle^2 - 2D_{xy}\langle V_x\rangle\langle V_y\rangle + D_{yy}\langle V_x\rangle 2 = E1 \quad (12)$$

$$D_{xx}[Y^A]^2 - 2D_{xy}X^AY^A + D_{yy}[X^A]^2 = E2 \quad (13)$$

$$D_{xx}\langle V_y\rangle Y^A - D_{xy}[\langle V_y\rangle X^A + \langle V_x\rangle Y^A] + D_{yy}\langle V_x\rangle X^A = E3 \quad (14)$$

7. Repeat steps 5 and 6 until Eq. 8 is satisfied.
8. Use the same procedure (steps 5–7) for any other observation well(s).

FIELD EXAMPLE

As part of the overall research program under NRC contract NRC-04-85-114, a research wellfield was completed in the northwest quarter of Section 16, T.25N, R.34E, six miles south of the town of Creston in Lincoln County, Washing-

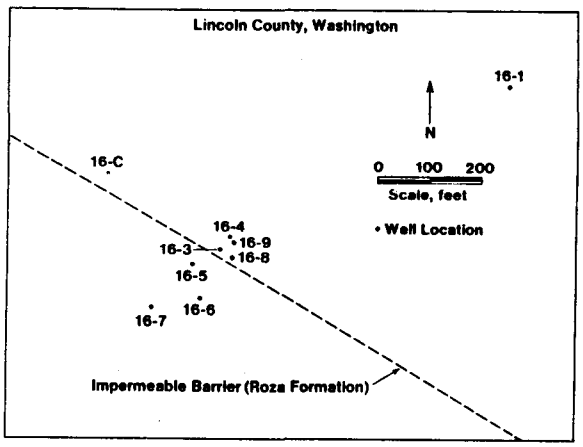

Fig. 2. Well location map.

ton (Fig. 2). Fig. 3 shows the general geologic cross-section of the study area. The Roza Member of the Wanapum Formation was selected as the target basalt for the study.[15] The Roza Member consists of two distinct flow horizons: the flow top and the flow interior. The flow top has much higher hydraulic conductivity and effective porosity, and is the main flow path for fluid transport.

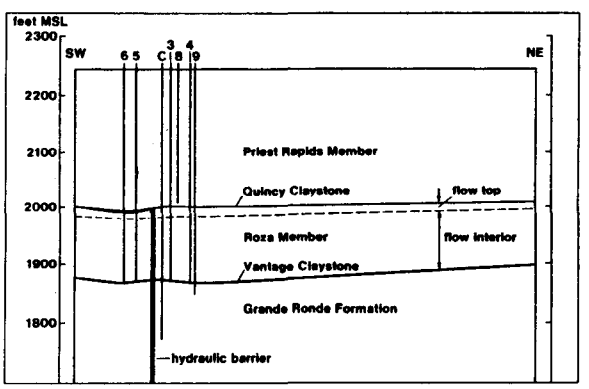

Fig. 3. Geologic cross-section.

Geologic and hydrologic evidence suggests the existence of a persistent linear hydraulic barrier trending northwest-southeast in the study area (Fig. 2). Regionally, the groundwater flow is southwesterly. Locally, however, the flow of groundwater on the north side of the hydraulic barrier changes from southwesterly to westerly.

As part of a program of hydrologic testing, a 29-day passive tracer test was performed between April 28 and May 26, 1987. A concentrated sodium chloride solution (total volume = 40 liters, total mass = 34.48 lb.) was released into the top opening (flow top of the Roza Member) of well 16-4. Fig. 4 is a schematic diagram of

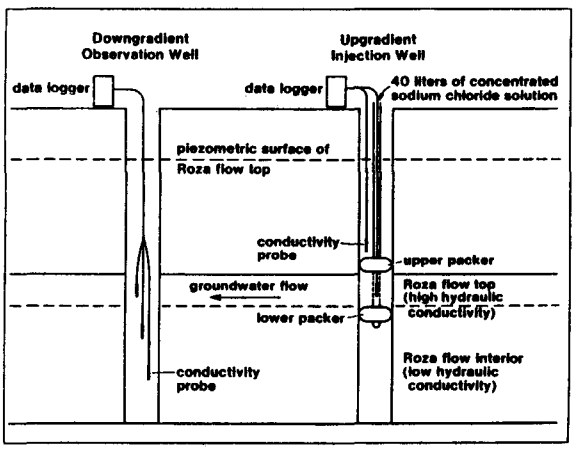

Fig. 4. Schematic diagram of tracer test.

the tracer test. The time vs. specific conductivity profile in downstream observation well 16-3 (Fig. 5) was measured using a set of downhole specific-conductivity probes and recorded by an automatic data logger. The specific conductivity values (in microSiemens per centimeter, μS/cm) were translated into concentration (in milligrams per liter, mg/l) based on laboratory calibration (1 μS/cm = 0.56 mg/l). The results of this tracer test were used to illustrate the procedure for calculating field-scale dispersion coefficients using de Josselin de Jong's theory.

Darcy's Law was first used to calculate the effective porosity of the Roza flow top. Based on the mean travel velocity of the tracer from well 16-4 to well 16-3 (30 ft/7.5 days), hydraulic conductivity (260 ft/day), and hydraulic gradient (0.09 ft/30 ft), the effective porosity of the Roza flow top was calculated to be 19 percent.[15]

Since the direction of local groundwater flow is affected by the geologic fault nearby and a precise direction of groundwater flow had not yet been determined, we initially assumed three possible groundwater flow directions in our cal-

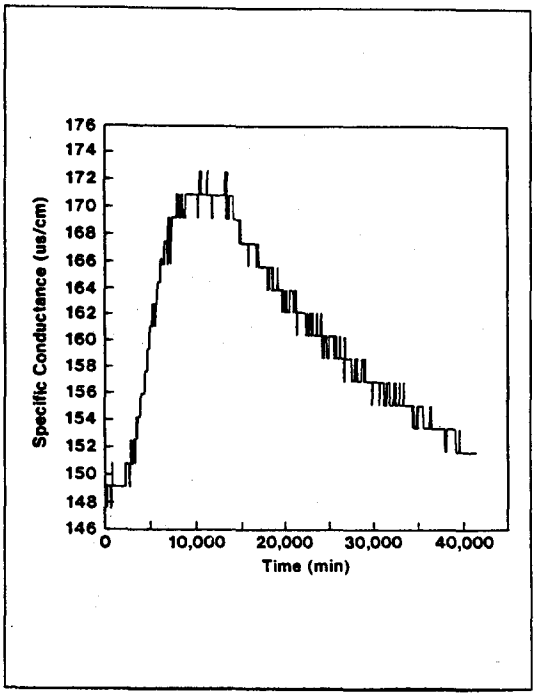

Fig. 5. Time/specific conductivity profile, downstream observation well 16-3.

culations. Table 1 summarizes the results.

During the tracer test, the specific conductivities of water in the Priest Rapids Formation (above the Roza flow top) and the Roza flow interior (below the Roza flow top) were also monitored, and leakage of the sodium chloride solution was detected. The exact amount of the leakage could not be determined accurately. In the first set of calculations, a leakage rate of 50 percent was assumed (Table 1). Further analysis indicated that the dispersivity values were not very sensitive to the mass of tracer used in the calculations (Table 2).

In making the assumption of Gaussian distribution, de Josselin de Jong was able to simplify Eq. 1 into three independent equations (Eqs. 5, 6, and 7 in the two-dimensional case). These three equations were used to calculate longitudinal and transverse dispersion coefficients and the direction of each. Using these values as input in Eq. 1, a good match was obtained (Fig. 6). The matched curve was almost identical regardless of which set of dispersivity values (those in Table 1 or those in Table 2) was used. Therefore, only one curve is shown in Fig. 6.

CONCLUSIONS

1. The proposed method provides a practical way to determine field dispersion coefficients from tracer tests. Since the tracer test is run in an undisturbed natural groundwater system, reliable field-scale values of dispersion coefficients can be obtained.
2. Because there is no induced injection or pumping during the tracer test, errors, arising in other methods from maintaining and measuring flow rate are eliminated.
3. The method allows us to calculate longitudinal as well as transverse coefficients, based upon the time-concentration curve from only one downstream observation well if we

Table 1. Dispersion Coefficients, Roza Flow Top Tracer Test

Groundwater flow		Dispersion coefficient (ft^2/d)		Dispersivity (ft)		Direction of longitudinal dispersivity
Assumed direction	Velocity (ft/d)	Longitudinal	Transverse	Longitudinal	Transverse	
S68°W	4.54	25.90	3.55	5.70	0.78	S62°W
S83°W	5.56	37.36	9.15	6.72	1.65	W
N82°W	7.86	142.88	12.43	18.18	1.58	N64°W

Note: It is assumed that 50% of the tracer remained in the flow top.

Table 2. Dispersion Coefficients, Roza Flow Top Tracer Test
(Direction of Groundwater Flow = S83°W)

Loss of tracer to nearby formations (%)	Tracer mass retained in flow top (lb/ft)	Dispersion coefficient (ft^2/d)		Dispersivity (ft)		Direction of longitudinal dispersivity
		Longi-tudinal	Trans-verse	Longi-tudinal	Trans-verse	
20%	2.52	36.05	7.91	6.48	1.42	S83°W
35%	2.05	36.16	8.42	6.50	1.51	S86°W
50%	1.61	37.36	9.15	6.72	1.65	W
65%	1.10	43.78	10.52	7.87	1.89	N82°W

have adequate knowledge of the groundwater flow.

4. The availability of reliable downhole specific conductivity probes and automatic data loggers makes the performance of long-term (several months) tracer test economically feasible.

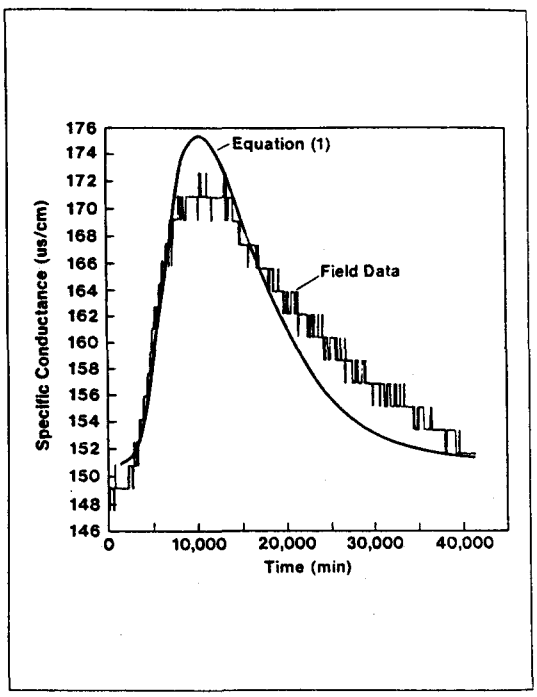

Fig. 6. Time/specific conductivity profiles, field data and match, downstream observation well 16-3.

APPENDIX

The following derivation was done by G. de Josselin de Jong in 1972 when he was a visiting professor at the New Mexico Institute of Mining and Technology. The original references are difficult to locate; thus it was decided to publish the detailed derivation in this appendix.

The concentration distribution C(X,Y,Z,T) due to the injection of a total amount of tracer mass M, at a point X=0, Y=0, Z=0, and time T, in an anisotropic porous medium is (eq. 12.2[8]):

$$C(X,Y,Z,T) = \frac{M}{\eta}\sqrt{\frac{||B||\langle t\rangle^3}{(2\pi T)^3}}\exp\left\{-\frac{1}{2}B_{kl}\frac{\langle t\rangle}{T}\left[X_k-\frac{\langle x_k\rangle}{\langle t\rangle}T\right]\cdot\left[X_l-\frac{\langle x_l\rangle}{\langle t\rangle}T\right]\right\}, \quad \text{(A. 1)}$$

where

C = concentration of injected tracer [ML^{-3}]

X,Y,Z = rectangular coordinates [L]

M = mass of injected tracer [M]

η = effective porosity

T = time [T]

$\langle x\rangle$ = average of x [L]

$\langle t \rangle$ = average of t [T]

B_{kl} is related to dispersion-coefficient tensor D_{ik} by Eq. A.2, and

$||B||$ is the determinant of tensor B_{kl} [L^{-2}].

$$D_{ik} B_{kl} \langle t \rangle = \frac{1}{2} \delta_{il}, \qquad \text{(A. 2)}$$

where subscripts i,k,l represent a set of coordinate systems. δ_{il} is Kroneker delta, where

$\delta_{il} = 1$ for $i = 1$,

$\delta_{il} = 0$ for $i \neq 1$.

The probability distribution is related to the tracer concentration by Eq. A.3:

$$P(X,Y,Z,T) = C(X,Y,Z,T) \times \frac{\eta}{M}, \qquad \text{(A. 3)}$$

Eq. A.1 therefore becomes

$$P(X,Y,Z,T) = \sqrt{\frac{||B|| \langle t \rangle^3}{(2\pi T)^3}} \exp \left\{ -\frac{1}{2} B_{kl} \frac{\langle t \rangle}{T} \left[x_k - \frac{\langle x_k \rangle}{\langle t \rangle} T \right] * \left[x_l - \frac{\langle x_l \rangle}{\langle t \rangle} T \right] \right\}. \qquad \text{(A. 4)}$$

Let us now consider T as the changing variable and compute the probability passing a point A with fixed coordinates X_k^A. Let the fixed quantities a,b,c be defined by

$$a = \frac{1}{2} B_{kl} \langle x_k \rangle \langle x_l \rangle \frac{1}{\langle t \rangle} \qquad \text{(A. 5a)}$$

$$b = B_{kl} x_k^A \langle x_l \rangle \qquad \text{(A. 5b)}$$

$$c = \frac{1}{2} B_{kl} x_k^A x_l^A \langle t \rangle \qquad \text{(A. 5c)}$$

Therefore, a is on the order of $1/\langle t \rangle$, b is on the order of N, and c is on the order of $N^2 \langle t \rangle$, where N is the average amount of steps for a particle to arrive at point A. Then Eq. A. 4 can be written for point A as

$$P^A(T) = \sqrt{\frac{||B||}{(2\pi)^3}} \exp \left\{ -\frac{3}{2} \ln \frac{T}{\langle t \rangle} - aT + b - \frac{c}{T} \right\}. \qquad \text{(A. 6)}$$

This expression is almost Gaussian in T, which can be seen by developing the argument of the exponent, i.e.,

$$\{ -(3/2) \ln (T/\langle t \rangle) - aT + b - (c/T) \}$$

is a Taylor series around its maximum.

Development of the argument in the exponent goes as follows: Let G(T) be the argument, such that

$$g(T) = \left\{ -aT - \frac{3}{2} \ln \frac{T}{\langle t \rangle} + b - \frac{c}{T} \right\} \qquad \text{(A. 7)}$$

Then we have

$$\frac{\partial g}{\partial T} = -a - \frac{3}{2T} + \frac{c}{T^2} \qquad \text{(A. 8)}$$

$$\frac{\partial^2 g}{\partial T^2} = + \frac{3}{2T^2} - \frac{2c}{T^3} \qquad \text{(A. 9)}$$

$$\frac{\partial^3 g}{\partial T^3} = -\frac{3}{T^3} + \frac{6c}{T^4} \qquad \text{(A. 10)}$$

The maximum occurs at T^A, such that

$$\frac{\partial g}{\partial T} [T=T^A] = 0 \qquad \text{(A. 11)}$$

or

$$aT^{A^2} + \frac{3}{2} T^A - c = 0, \qquad \text{(A. 12)}$$

giving the only useful root

$$T^A = -\frac{3}{4a} + \frac{1}{2a} \sqrt{\frac{9}{4} + 4ac}. \qquad \text{(A. 13)}$$

Since (ac) is on the order of N^2, the factor 9/4 can be disregarded. Therefore,

$$T^A = -\frac{3}{4a} + \sqrt{\frac{c}{a}}. \qquad \text{(A. 14)}$$

Eq. A. 14 can be further approximated by Eq. A. 15 because $\sqrt{c/a}$ is on the order of $N \langle t \rangle$ and $3/4a$ is on the order of $\langle t \rangle$:

$$T^A = \sqrt{\frac{c}{a}}. \qquad \text{(A. 15)}$$

Because

$$\frac{\partial^2 g}{\partial T^2}\left(T=T^A\right)$$

can be written

$$\frac{1}{\left(T^A\right)^3}\left[\frac{3}{2}T^A - 2c\right],$$

use of Eq. A. 12 gives

$$\frac{\partial^2 g}{\partial T^2}\left(T^A\right) = \frac{1}{\left(T^A\right)^3}\left[-c - a{T^A}^2\right] =$$

$$\sqrt{\frac{a^3}{c^3}}\left[-c - a\frac{c}{a}\right] = -2a\sqrt{\frac{a}{c}}. \quad \text{(A. 16)}$$

The Taylor expansion of g(T) around T^A can now be written as

$$g(T) = g\left(T^A\right) + \frac{\partial g(T)}{\partial T}\left(T=T^A\right)\left(T-T^A\right) + \frac{\partial^2 g(T)}{2!\,\partial T^2}\left(T=T^A\right)\left(T-T^A\right)^2 + \cdots \quad \text{(A. 17)}$$

Since

$$\frac{\partial g(T)}{\partial T}\ [T=T^A]$$

is made zero, this becomes, by use of Eqs. A. 7, A. 15, and A. 16,

$$g(T) = \left[b - 2\sqrt{ac} - \frac{3}{2}\ln\frac{T^A}{\langle t\rangle}\right] - a\sqrt{\frac{a}{c}}\left(T - T^A\right)^2 + \cdots, \quad \text{(A. 18)}$$

where the third-order term can be disregarded, being an order of magnitude smaller than the second-order term. Hence, g(T) becomes

$$g(T) = b - 2\sqrt{ac} - a\sqrt{\frac{a}{c}}\left(T - T^A\right)^2 \cdots - \frac{3}{2}\ln\frac{T^A}{\langle t\rangle}. \quad \text{(A. 19)}$$

So the probability distribution (Eq. A. 6) can be written as

$$P^A(T) = \sqrt{\frac{\|B\|\langle t\rangle^3}{(2\pi T^A)^3}}\exp\left[b - 2\sqrt{ac}\right] * \exp\left\{-a\sqrt{\frac{a}{c}}\left(T-T^A\right)^2\right\}. \quad \text{(A. 20)}$$

This is a Gaussian distribution with

Peak value of probability

$$P^A(T)_{peak} = \sqrt{\frac{\|B\|\langle t\rangle^3}{(2\pi T^A)^3}}\exp\left[b - 2\sqrt{ac}\right] \quad \text{(A. 21)}$$

Peak value of concentration

$$C^A(T)_{peak} = \frac{M}{\eta}\sqrt{\frac{\|B\|\langle t\rangle^3}{(2\pi T^A)^3}}\exp\left[b - 2\sqrt{ac}\right] \quad \text{(A. 22)}$$

Time of peak $\quad T^A = \sqrt{\frac{c}{a}} \quad \text{(A. 23)}$

Standard deviation $\quad \sigma^A = \sqrt{\frac{1}{2a}\sqrt{\frac{c}{a}}} \quad \text{(A. 24)}$

The values $C^A(T)_{peak}$, T^A, and σ^A can be obtained from measurements from field observations for a tracer test (Fig. 1).

From Eqs. A. 23 and A. 24, we find

$$a = \frac{T^A}{2[\sigma^A]^2} \quad \text{(A. 25)}$$

giving, in conjunction with Eq. A. 5 and the inversion for B,

$$\frac{T^A}{2[\sigma^A]^2} = B_{kl}\frac{\langle x_k\rangle\langle x_1\rangle}{2\langle t\rangle}. \quad \text{(A. 26)}$$

Furthermore, using Eqs. A. 23 and A. 25, we find

$$c = \frac{[T^A]^3}{2[\sigma^A]^2}, \quad \text{(A. 27)}$$

giving, in conjunction with Eq. A. 5,

$$\frac{[T^A]^3}{2[\sigma^A]^2} = B_{kl}\frac{x_k^A\, x_1^A}{2}\langle t\rangle. \quad \text{(A. 28)}$$

Finally, using Eqs. A. 23 and A. 27 in Eq. A. 22, we find

$$\frac{M}{\eta}\sqrt{\|B\|\langle t\rangle^3}\exp\langle b\rangle = c^A_{peak}\sqrt{(2\pi T^A)^3}\exp\left\{\left[\frac{T^A}{\sigma^A}\right]^2\right\}. \quad \text{(A. 29)}$$

The unknowns are B_{kl}, $\langle x_k\rangle/\langle t\rangle$, and $\langle x_1\rangle/\langle t\rangle$.

In the two-dimensional case, the inversion of B can be written as

$$B_{xx} = \frac{D_{yy}}{2\langle t\rangle \|D\|} \qquad B_{xy} = \frac{-D_{xy}}{2\langle t\rangle \|D\|}$$

$$B_{xy} = B_{yx} \qquad B_{yy} = \frac{D_{xx}}{2\langle t\rangle \|D\|} \qquad \text{(A. 30)}$$

Taking further into account that the factor 3 appearing under the root in the expression for P (Eqs. A. 4 and A. 21) was the number of dimensions the following formula would be for two dimensions:

$$C(X,Y,T) = \frac{M}{\eta}\sqrt{\frac{\|B\|\langle t\rangle^2}{(2\pi T)^2}}\exp\left\{-\frac{1}{2}B_{kl}\frac{\langle t\rangle}{T}\left[X_k - \frac{\langle x_k\rangle}{\langle t\rangle}T\right]\cdot\left[X_l - \frac{\langle x_l\rangle}{\langle t\rangle}T\right]\right\}. \qquad \text{(A. 31)}$$

So the system is as follows:

$$\frac{T^A}{2(\sigma^A)^2} = \frac{1}{4\|D\|}\left[D_{xx}\langle v_y\rangle^2 - 2D_{xy}\langle v_x\rangle\langle v_y\rangle + D_{yy}\langle v_x\rangle^2\right] \qquad \text{(A. 32)}$$

$$\frac{(T^A)^3}{2(\sigma^A)^2} = \frac{1}{4\|D\|}\left[D_{xx}(Y^A)^2 - 2D_{xy}X^AY^A + D_{yy}(X^A)^2\right] \qquad \text{(A. 33)}$$

$$C^A_{peak}(2\pi T^A)\exp\left\{\left[\frac{T^A}{\sigma^A}\right]^2\right\} = \frac{M}{\eta}(4\|D\|)^{-1/2}$$

$$\exp\left\{\frac{\left[D_{xx}\langle v_y\rangle Y^A - D_{xy}\left[\langle v_y\rangle X^A + \langle v_x\rangle Y^A\right] + D_{yy}\langle v_x\rangle X^A\right]}{2\|D\|}\right\}. \qquad \text{(A. 34)}$$

The unknowns are D_{xx}, D_{xy}, D_{yy}, $\langle V_x\rangle$, $\langle V_y\rangle$, and η, where $\langle V_x\rangle$ and $\langle V_y\rangle$ are the x and y components of groundwater velocity.

ACKNOWLEDGEMENTS

This work was supported by the U.S. Nuclear Regulatory Commission under contract NRC-04-85-114. The NRC project manager was Timothy J. McCartin and In-Situ Inc.'s project manager was Timothy D. Steele.

The authors express appreciation to Jim Paschis for drilling supervision and geologic studies; to John E. Benedik, Jr., for conducting the tracer test; to Robert A. Koenig for performing aquifer tests; and to Jane M. Reverand for preparing the manuscript.

REFERENCES

1. Bear, J., and Y. Bachmat. A generalized theory on hydrodynamic dispersion in porous media. Int. Assoc. Sci. Hydrol., Symposium on Artificial Recharge and Management of Aquifers, Haifa, Israel. IASH Pub. No. 72, pp. 7-16, 1967.
2. Gelhar, L. W., A. L. Gutjahr, and R. L. Naff. Stochastic analysis of macrodispersion in a stratified aquifer. Water Resour. Res., 15: 1387-1397, 1979.
3. Gelhar, L. W., and C. J. Axness. Three-dimensional stochastic analysis of macro-dispersion in aquifers. Water Resour. Res., 19: 161-180, 1983.
4. Winter, C. L., S. P. Neuman, and C. M. Newman. Prediction of far-field subsurface radionuclide dispersion coefficients from hydraulic conductivity measurements. Dept. of Hydrology and Water Resources, Univ. of Arizona, Tucson; report for U.S. Nuclear Regulatory Commission, NUREG/CR-3612, 1984.
5. Neuman, S. P., C. L. Winter, and C. M. Newman. Stochastic theory of field-scale Fickian dispersion in anisotropic porous media. Water Resour. Res., 23: 453-466, 1987.
6. de Josselin de Jong, G. Longitudinal and transverse diffusion in granular deposits. Trans. Amer. Geophys. Union, 39: 67-174, 1958.
7. de Josselin de Jong, G. The tensor character of the dispersion coefficient in anisotropic porous media. Proceedings, IAHR Symposium, Haifa, pp. 259-267, 1969.
8. de Josselin de Jong, G. Dispersion of a point injection in an anisotropic porous medium. Geoscience Dept., New Mexico Inst. of Mining & Technology, Socorro, NM, 1972.
9. de Josselin de Jong, G., and S. C. Way. Dispersion in fissured rock. Geoscience Dept., New Mexico Inst. of Mining & Technology, Socorro, NM, 1972.
10. Way, S. C., and C. R. McKee. Restoration of in-situ coal gasification sites from naturally occurring groundwater flow and dispersion. In Situ, 5(2): 77-101, 1981.
11. Endo, H. K., J. C. S. Long, C. R. Wilson, and

P. A. Witherspoon. A model for investigating mechanical transport in fracture networks. Water Resour. Res., 20: 1390-1400, 1984.
12. Schwartz, F. W., L. Smith, and A. S. Crowe. A stochastic analysis of macroscopic dispersion in fractured media. Water Resour. Res., 19: 1253-1265, 1983.
13. Sposito, G. W. A. Jury, and V. K. Gupta. Fundamental problems in the stochastic convection-dispersion model of solute transport in aquifers and field soils. Water Resour. Res., 22: 77-88, 1986.
14. Sudicky, E. A., J. A. Cherry, and E. O. Frind. Migration of contaminants in groundwater at a landfill, 4: A natural-gradient dispersion test. In: J. A. Cherry (guest ed.), Migration of Contaminants in Groundwater at a Landfill: A Case Study. J. Hydrology, 63: 81-108, 1983.
15. Steele, T. D., J. A. Paschis, and R. A. Koenig. Hydrogeologic characterization of basalts of the northern rim of the Columbia Plateau physiographic province and of the Creston study area, eastern Washington. Report for U.S. Nuclear Regulatory Commission, NUREG/CR-5107, 1988.

收稿日期：民國80年10月30日
修正日期：民國80年11月13日
接受日期：民國80年11月17日